

Technical Data on ORIENTCORE HI-B™

NIPPON STEEL NORTH AMERICA, INC.

New York	1251 Ave of the Americas, Suite 2320, New York, NY, U.S.A. 10020-0080 TEL:+1-212-486-7150/FAX:+1-212-593-3049
Chicago	900 North Michigan Av., Suite 1820, Chicago, Illinois 60611, U.S.A. TEL:+1-312-751-0800/FAX:+1-312-751-0345
Houston	945 Bunker Hill Suite 600, Houston, Texas 77024, U.S.A. TEL:+1-713-654-7111/FAX:+1-713-654-1261
Mexico	Calle de Ruben Dario 281 No.2101, Colonia Bosque de Chapultepec, Mexico, D. F. 11580, Mexico TEL:+52-55-5281-6123/FAX:+52-55-5280-0501

NIPPON STEEL AMÉRICA DO SUL LTDA.

Sao Paulo	Avenida Paulista 2300, 18º andar conj. 181 e 183 CEP 01310-300, São Paulo, SP, Brasil TEL:+55-11-3563-1900/FAX:+55-11-3563-1901
Belo Horizonte	Av. do Contorno, 6594-13º andar-Sala1302, Lourdes, Belo Horizonte-MG, CEP 30110-044, Brasil TEL:+55-31-2191-4000/FAX:+55-31-2191-4880

NIPPON STEEL CORPORATION European Office

Duesseldorf	Am Seestern 8, 40547 Duesseldorf Federal Republic of Germany TEL:+49-211-5306680/FAX:+49-211-5961163
--------------------	---

NIPPON STEEL CORPORATION Dubai Office

Dubai	JAFZA16, Office No.613 Jebel Ali Free Zone, Dubai, U.A.E. (PO Box : 18347) TEL:+971-4-887-6020/FAX:+971-4-887-0206
--------------	--

NIPPON STEEL AUSTRALIA PTY. LIMITED

Sydney	Level 5, 20 Hunter Street, Sydney, N.S.W. 2000, Australia TEL:+61-2-8036-6600/FAX:+61-2-9221-5277
---------------	--

NIPPON STEEL INDIA PRIVATE LIMITED

New Delhi	Prius Platinum, A Wing, Ground Floor, D-3, Dist. Centre, Saket, New Delhi -110017, INDIA TEL:+91-11-4763-0000/FAX:+91-11-4763-0001
------------------	--

NIPPON STEEL CONSULTING (BEIJING) CO.,LTD.

Beijing	Room No.5002, Chang Fu Gong Center, Jian Guo Men Wai Da Jie 26, Chaoyang District Beijing, 100022, P.R. China TEL:+86-10-6513-8593/FAX:+86-10-6513-7197
Shanghai	Room No.808, UNITED PLAZA, 1468 Nanjing Road West, Jingan District Shanghai, 200040, P.R. China TEL:+86-21-6247-9900/FAX:+86-21-6247-1858
Guangzhou	Room No.1402 G.T.Land Plaza D Tower, No.8 Zhujiang West Road, Zhujiang New Town, Tianhe District Guangzhou. 510623, P.R.China TEL:+86-20-8386-8178/FAX:+86-20-8386-7066

NIPPON STEEL SOUTHEAST ASIA PTE. LTD.

Singapore	16 Raffles Quay #17-01 Hong Leong Building, Singapore 048581 TEL:+65-6223-6777/FAX:+65-6224-4207
------------------	---

PT. NIPPON STEEL INDONESIA

Jakarta	Sentral Senayan II 201-2C Ground floor, Jl. Asia Afrika No. 8, Gelora Bung Karno-Senayan, Jakarta Pusat 10270, Indonesia TEL:+62-21-290-39210/FAX:+62-21-290-39211
----------------	--

NIPPON STEEL (THAILAND) CO., LTD.

Bangkok	909 Ample Tower 14th, Debaratana Road, Khwang Bangna, Khet Bangna, Bangkok, 10260, Thailand TEL:+66-2-744-1480-3/FAX:+66-2-744-1485
----------------	---

NIPPON STEEL VIETNAM COMPANY LIMITED

Ho Chi Minh City	Room 2001, 20th Floor, Sunwah Tower 115 Nguyen Hue Blvd, Ben Nghe Ward, Dist.1, Hochiminh City, Vietnam TEL:+84-28-3914-7016/FAX:+84-28-3914-7018
Ha Noi	Room 402 4th floor Corner Stone Building 16 Phan Chu Trinh, Hoan Kiem, Ha Noi, Vietnam TEL:+84-24-3633-2029

NIPPON STEEL THAI SUMILOX CO.,Ltd.

	1/79 Moo 5, Rojana Industrial Park, Rojana Road Thamnon Kanham, Amphur U-Thai, Ayutthaya 13210, Thailand TEL: +66-35-227-044/FAX:+66-35-227-055
--	---

CONTENTS

1. General Information	2
1-1 HI-B Grain-Oriented Silicon-Iron	
1-2 Magnetic Properties of ORIENTCORE•HI-B™	
1-3 Measuring Apparatus	
2. Typical Characteristics of ORIENTCORE•HI-B™ Cores in Commercial Transformers	11
3. Building Factor of Commercial Transformers	12
4. Core Loss Characteristics of Model Transformer	14
4-1 Single-Phase Model Transformer	
4-2 3-Phase Model Transformer	
APPENDIX [I] A New Instrument for Measuring Local Core Losses Using Thermistor Bridge	20
APPENDIX [II] Various Core Stacking Types (3ϕ)	23
APPENDIX [III] Mechanical and Physical Properties of HI-B and C.G.O.	24
<p style="margin: 0;">Note: HI-B = ORIENTCORE•HI-B™ C.G.O. = Conventional Grain-Oriented Electrical Steel Sheet (ORIENTCORE)</p>	

Notice: While every effort has been made to ensure the accuracy of the information contained within this publication, the use of the information is at the reader's risk and no warranty is implied or expressed by NIPPON STEEL CORPORATION with respect to the use of the information contained herein. The information in this publication is subject to change or modification without notice. Please contact the NIPPON STEEL CORPORATION office for the latest information. Please refrain from unauthorized reproduction or copying of the contents of this publication. The names of our products and services shown in this publication are trademarks or registered trademarks of NIPPON STEEL CORPORATION, affiliated companies, or third parties granting rights to NIPPON STEEL CORPORATION or affiliated companies. Other product or service names shown may be trademarks or registered trademarks of their respective owners.

1. General Information

1-1 HI-B Grain-Oriented Silicon-Iron

A new type of grain-oriented silicon-iron has been developed by NIPPON STEEL Corp.. It is called ORIENTCORE·HI-B, commonly abbreviated to HI-B. The properties of this material enable the production of transformers with reduced core loss, exciting current and noise. In addition, transformers with a higher efficiency, larger capacity and more compact design are possible with HI-B.

The main difference between HI-B and conventional material (C.G.O.) is that a higher degree of grain orientation is obtained in HI-B, as shown in Fig. 1-1-1. The average deviations of $\langle 001 \rangle$ axis from the rolling direction are about 3° in HI-B and about 7° in C.G.O..

However, it should be noted that there is also a difference in the tensile effects due to the surface coating which consists of a glass-film and a phosphate coating (see Fig. 1-1-2). The surface coating not only acts as interlaminar insulation, but also places the material under tensile stress in the rolling direction.

The improvement in grain orientation has resulted in an improvement in the magnetizing characteristics, a decrease of hysteresis loss (see Fig. 1-1-3) and a reduction of eddy current loss with applied tensile stress for the materials as shown in Fig. 1-1-4. The reduction in magnetostriction (see Fig. 1-1-5), should result in a reduction in transformer noise.

In commercial practice, tensile stress in the material originates from the difference in thermal expansion coefficients between the surface coating and the steel. The reduction of the losses by tensile stress, which is produced in the material by the surface coating, is shown in Fig. 1. 1. 7. The values of tensile stress in the rolling direction are about $0.3\sim 0.5 \text{ kg/mm}^2$ for stress coating (S-coating) and about $0.1\sim 0.2 \text{ kg/mm}^2$ for conventional coating. The decrease in losses is remarkable in HI-B with S-coating. The reduction of losses due to surface coating (produce isotropic tensile stress in the material) is almost the same as that at the corresponding value of tensile stress applied along the rolling direction. This shows that the effect of tensile stress due to surface coating on magnetic properties may be attributed to the anisotropic property of magnetostriction in Goss textured silicon-iron (see Fig. 1-1-2 (a)).

1-2 Magnetic Properties of ORIENTCORE·HI-B

1-2-1 Core Loss and Permeability

As the B-W curves in Fig. 1-2-1 show, ORIENTCORE·HI-B exhibits markedly improved core loss characteristics. The B-H curves in Fig. 1-2-2 indicate that ORIENTCORE·HI-B has high permeability, with saturation induction comparable to that of conventional material.

1-2-2 Polydirectional Properties

Since ORIENTCORE·HI-B features excellent grain orientation, it has superior magnetic properties in the rolling direction. However, its magnetic properties around the transverse direction are inferior to those of conventional material (Fig. 1-2-3).

1-2-3 Stress Sensitivity

When grain-oriented electrical steel sheet is being fabricated into transformer cores, stresses are induced in the core. While elastic tensile stress has a favorable effect on magnetostriction characteristics, compressive stress has a deleterious effect (Fig. 1-2-4). Because of the effect of S-coating, ORIENTCORE·HI-B is less affected by compressive stress than C.G.O.. ORIENTCORE·HI-B is also less sensitive to slitting, shearing, punching, bending and other kinds of stress (Figs. 1-2-5, 1-2-6, 1-2-7 and 1-2-8).

1-3 Measuring Apparatus

Fig. 1-3-1 shows a single sheet tester for measuring losses and permeabilities. This apparatus produces measured values that correlate well with the Epstein test (see Fig. 1-3-2) and is useful for testing under applied tensile or compressive stress.

Fig. 1-3-3 shows the a.c.magnetostriction tester which features a differential transformer for detecting a.c.magnetostrictive vibration. This apparatus is also useful for testing under applied tensile or compressive stress.

Fig. 1-3-4 shows the instrument for measuring losses under elastic bending.

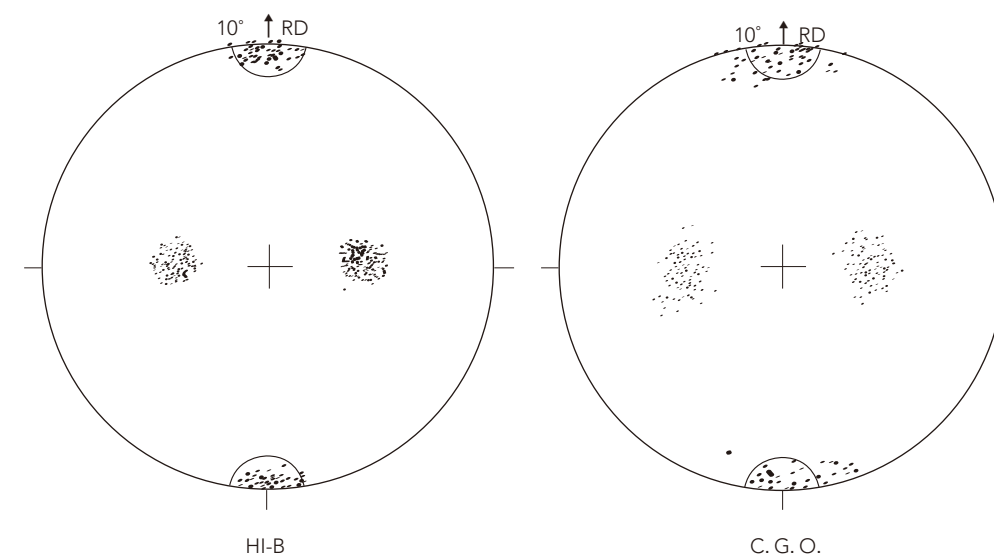


Fig. 1-1-1 (100) pole figures showing the grain orientation of HI-B and C.G.O.

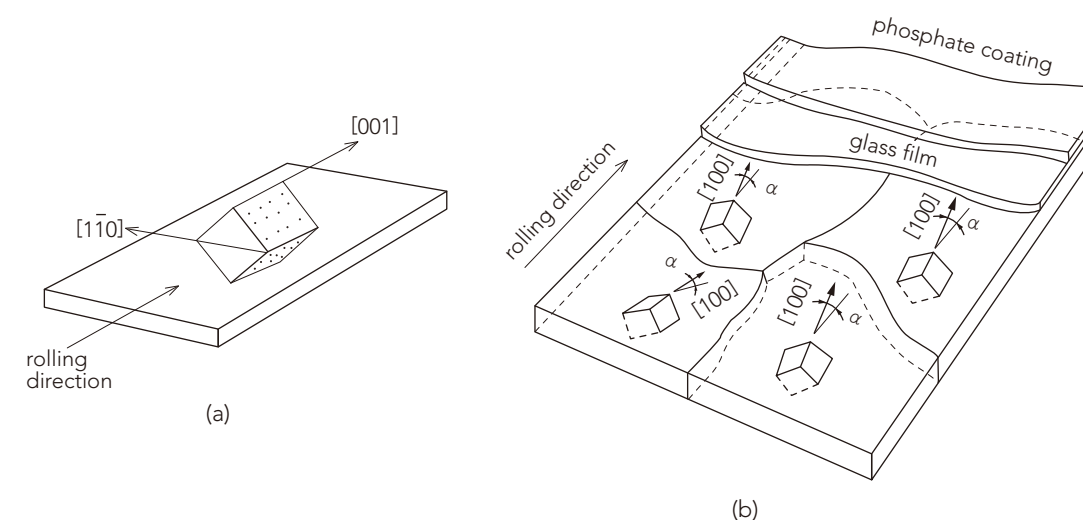


Fig. 1-1-2 Schematic diagram showing (a) Goss oriented texture and (b) surface coating.

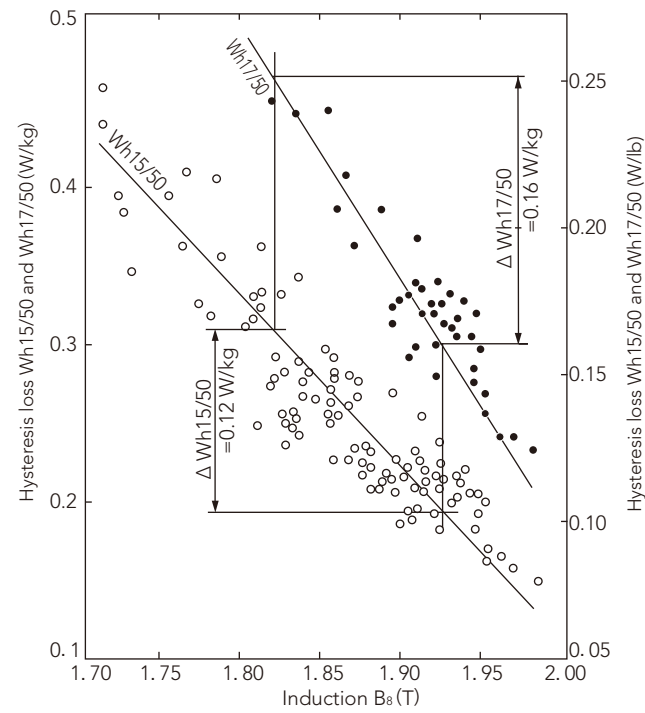


Fig. 1-1-3 Effects of B_s (Induction at magnetizing force of 800 A/m) value on hysteresis loss.

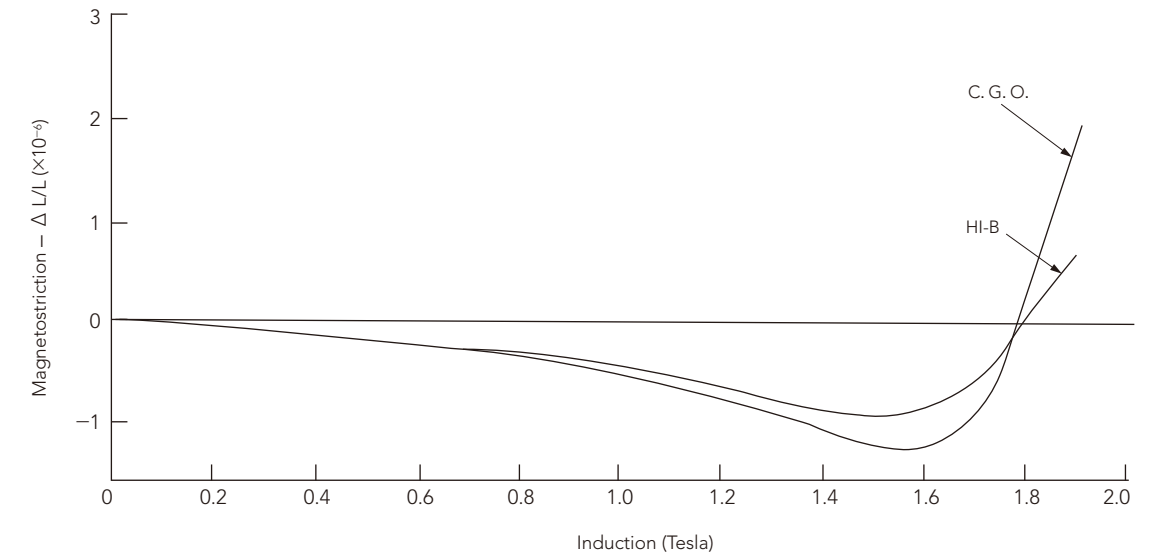


Fig. 1-1-5 A.C. magnetostriction (O-P) curves for HI-B and C.G.O. magnetized at 60 Hz applied tensile stress free.

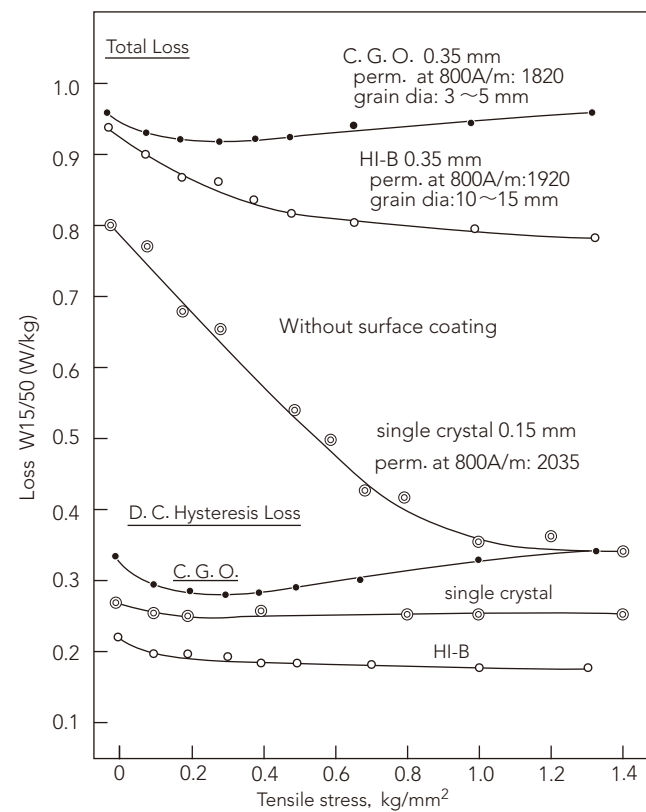


Fig. 1-1-4 Effect of the degree of grain orientation on the tensile stress dependence of losses for grain-oriented silicon steel.

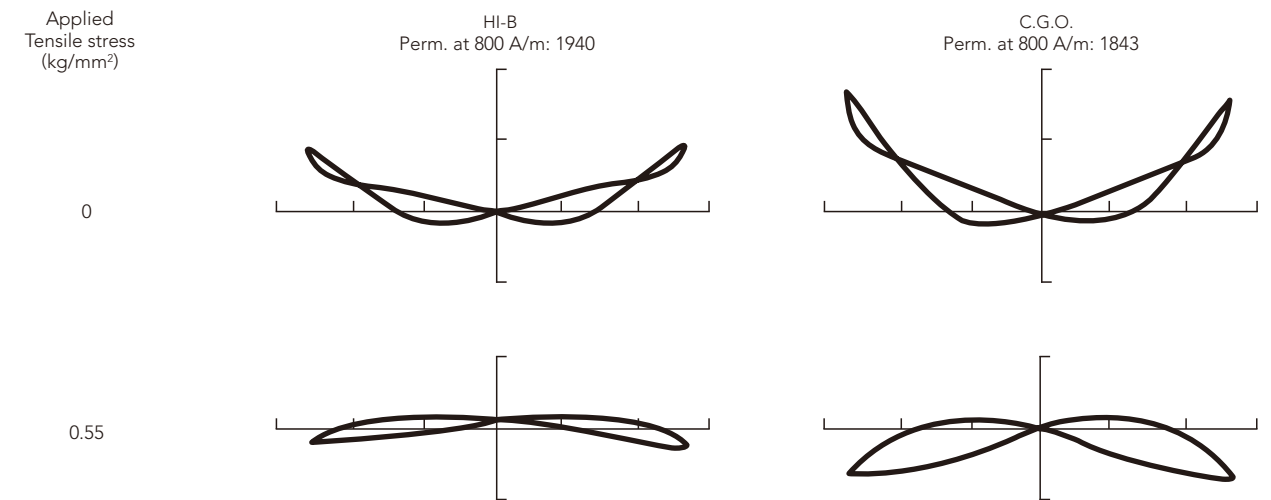


Fig. 1-1-6 Effect of applied tensile stress on magnetostriction characteristics at 60 Hz for HI-B and C.G.O. without surface coating.
Thickness: 0.30 mm.
Abscissa: flux density, maximum flux density=1.7 T
Ordinate: fractional change in length 1 div= 1.44×10^{-6}

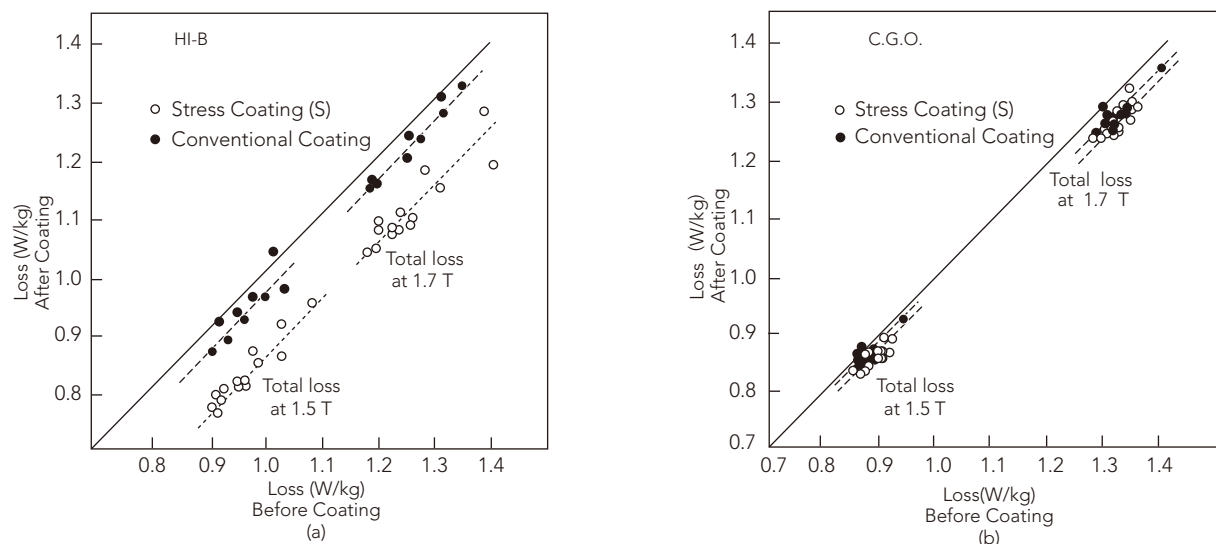


Fig. 1-1-7 Effect of phosphate coatings on losses measured at 50 Hz for grain-oriented 3% Si-Fe. Phosphate coating are coated after removal of glass-film.
 (a) HI-B, thickness: 0.30 mm, grain diameter: 10~15 mm, average permeability at 800 A/m: 1920
 (b) C.G.O., thickness: 0.30 mm, grain diameter: 3~5 mm, average permeability at 800 A/m: 1820

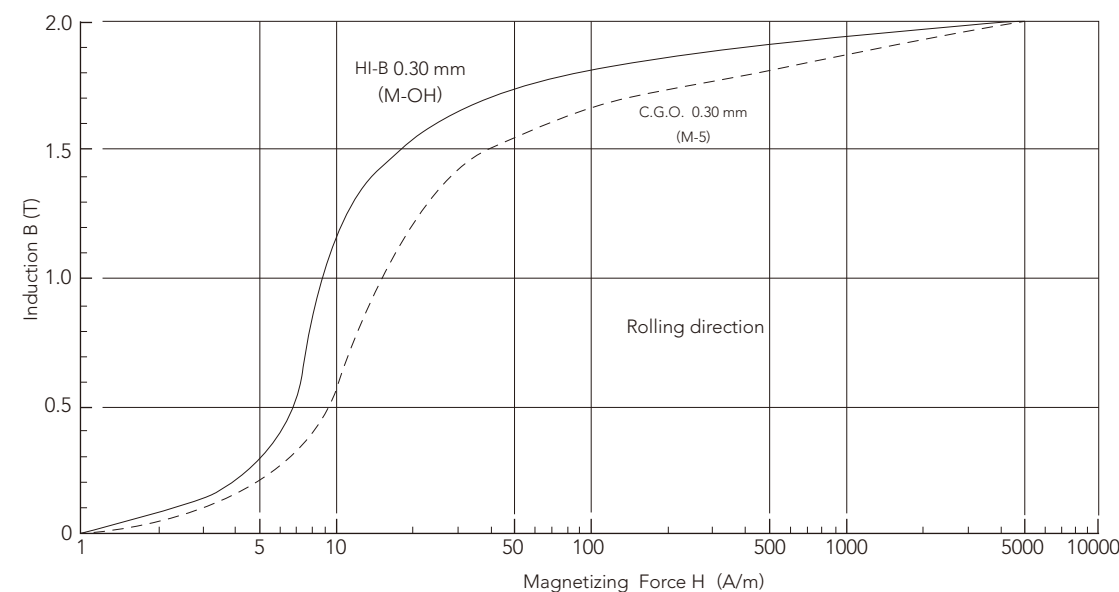


Fig. 1-2-2 Comparison of D.C. B-H curves between HI-B and C.G.O.

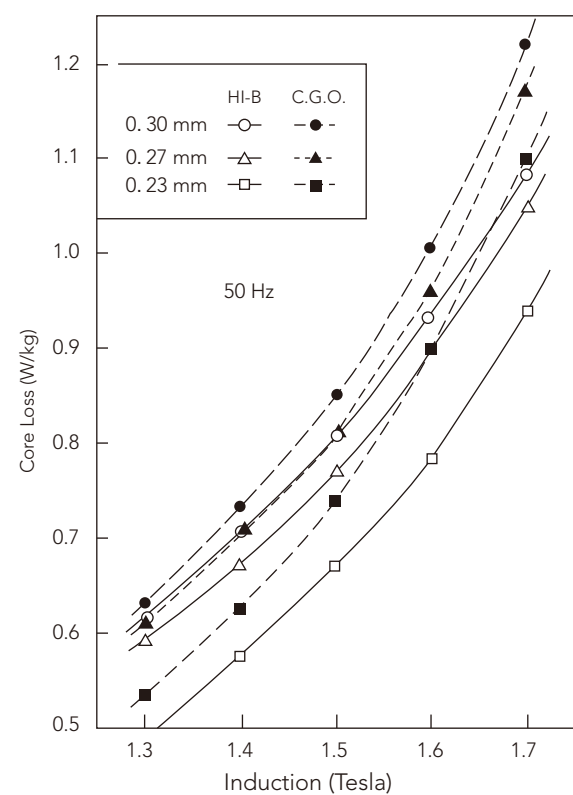


Fig. 1-2-1 Comparison of core loss curves between HI-B and C.G.O.

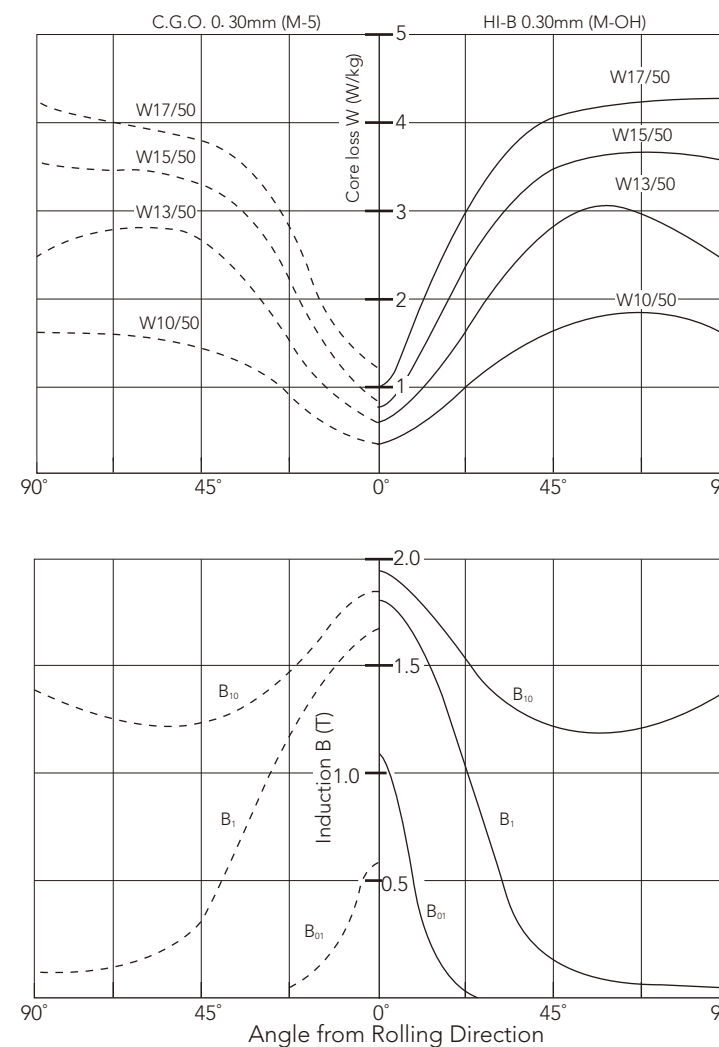


Fig. 1-2-3 Angle dependence of core loss and induction for HI-B and C.G.O.

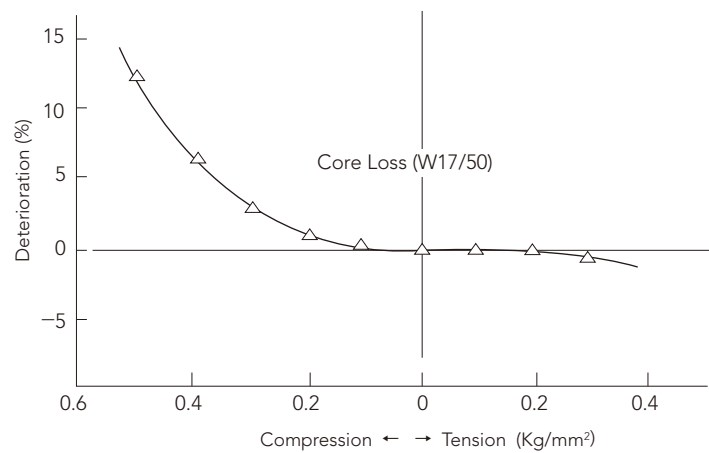


Fig. 1-2-4(a) Relation between stress and core loss for HI-B (0.30 mm)

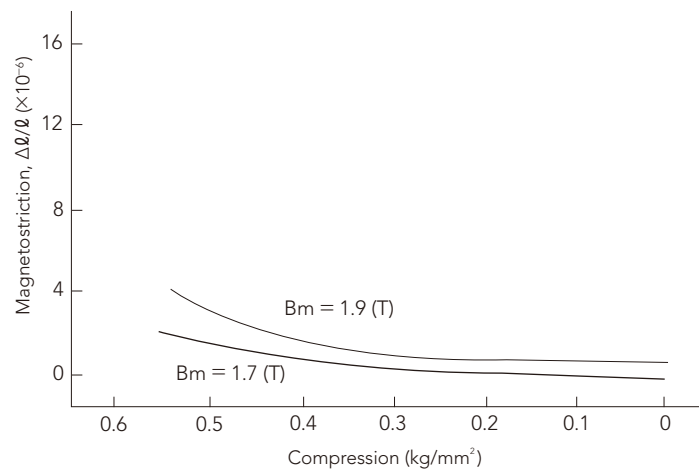


Fig. 1-2-4(b) Effect of compressive stress on magnetostriction (O-P) for HI-B magnetized at 60 Hz

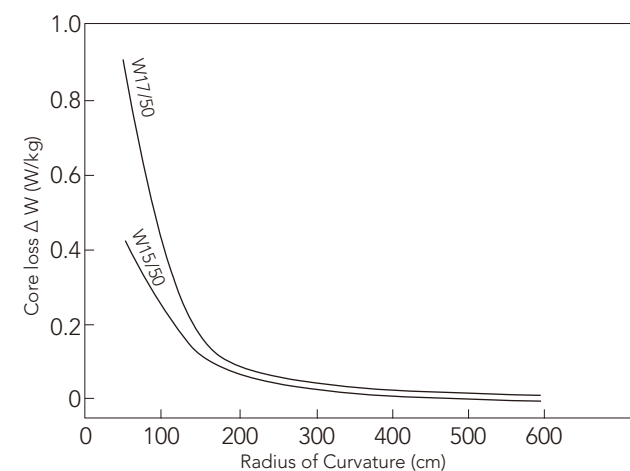


Fig. 1-2-7 Effect of elastic bending on core loss for HI-B (0.30 mm) (Measurements were taken according to Fig. 1-3-4)

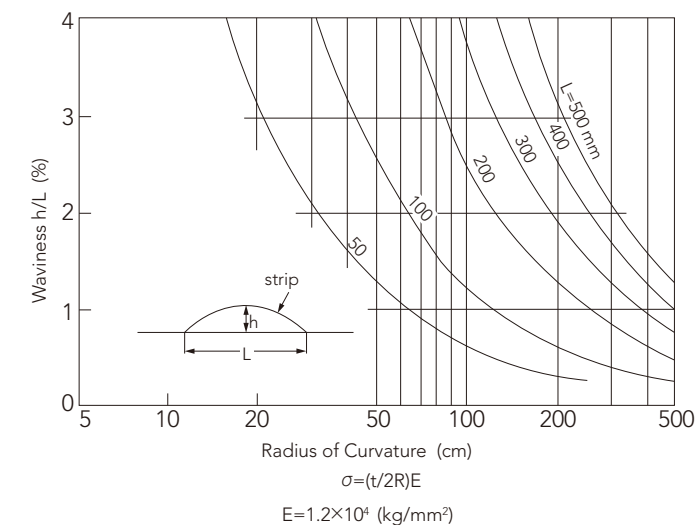


Fig. 1-2-8 Relation between maximum stress and radius of curvature in elastic bending.

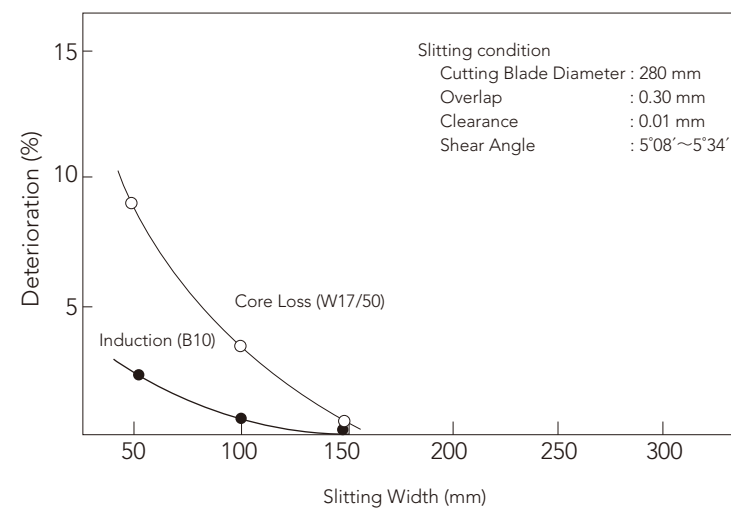


Fig. 1-2-5 Effect of slitting on magnetic properties for HI-B (0.30 mm)

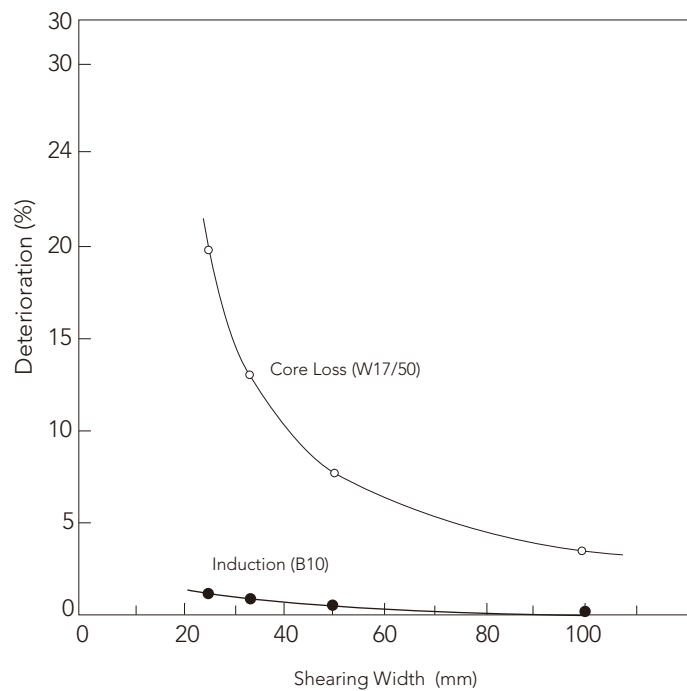


Fig. 1-2-6 Effect of shearing on magnetic properties for HI-B (0.30 mm)

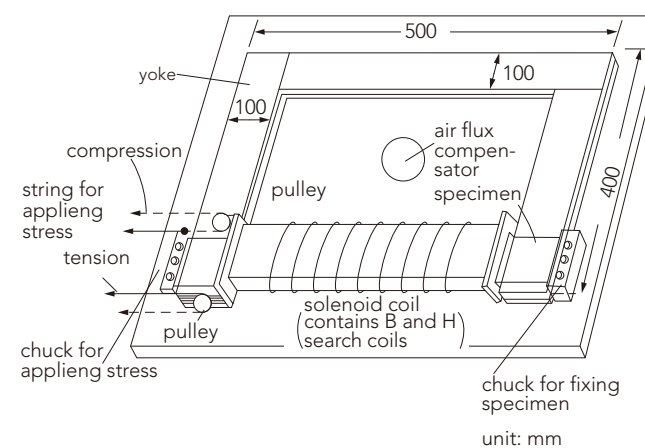


Fig. 1-3-1 Apparatus for stress-loss determination.

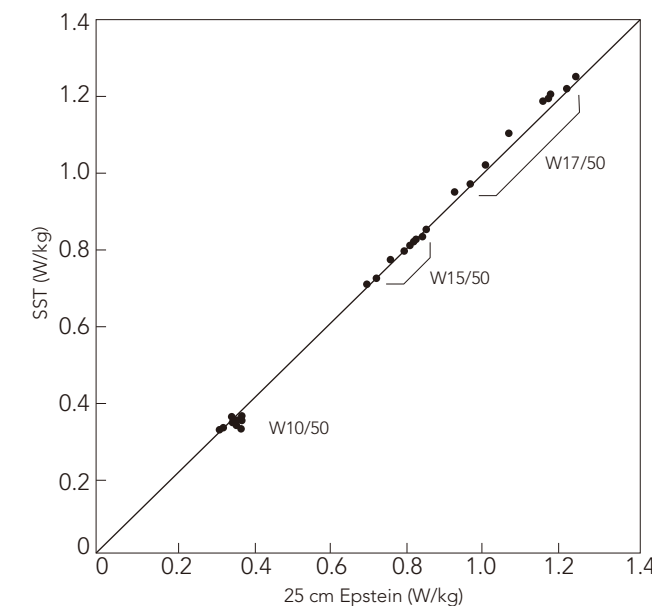


Fig. 1-3-2 Comparison of loss values measured by single strip tester and 25 cm Epstein tester.

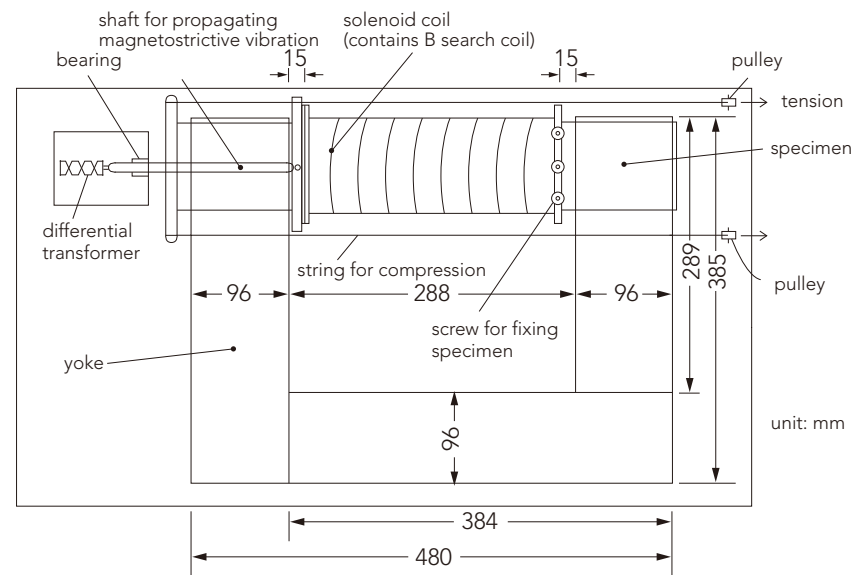


Fig. 1-3-3 Apparatus for compressive stress- σ , c , magnetostriction determination.

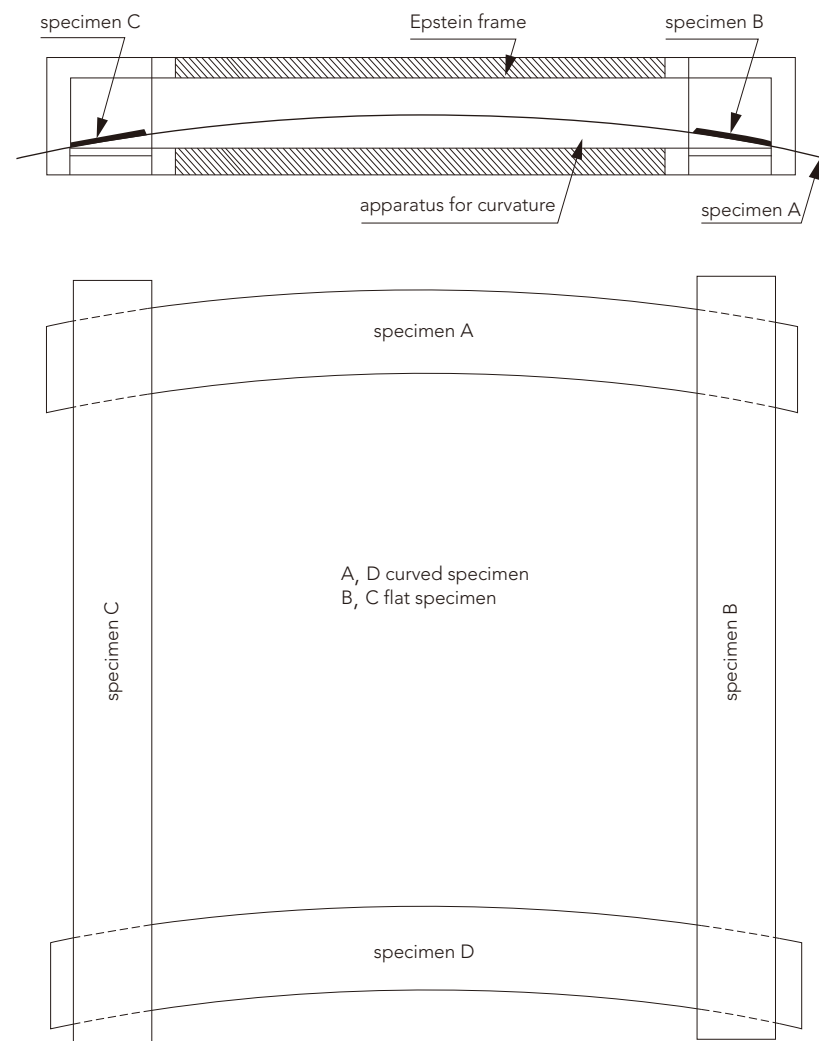


Fig. 1-3-4 Equipment that gives curvature to Epstein specimens in 25 cm Epstein-frame.

2. Typical Characteristics of ORIENTCORE•HI-B Cores in Commercial Transformers

ORIENTCORE•HI-B is supplied to electrical machinery manufacturers both in Japan and the other countries for use in transformers ranging from 10 KVA wound core transformers to ultra-large 1,000 MVA stacked core transformers. Data from manufacturers indicate that ORIENTCORE•HI-B offers a 5~20 per cent reduction in core loss, a 10~50 per cent reduction in exciting volt-ampere, and a 2~7 dB reduction in noise.

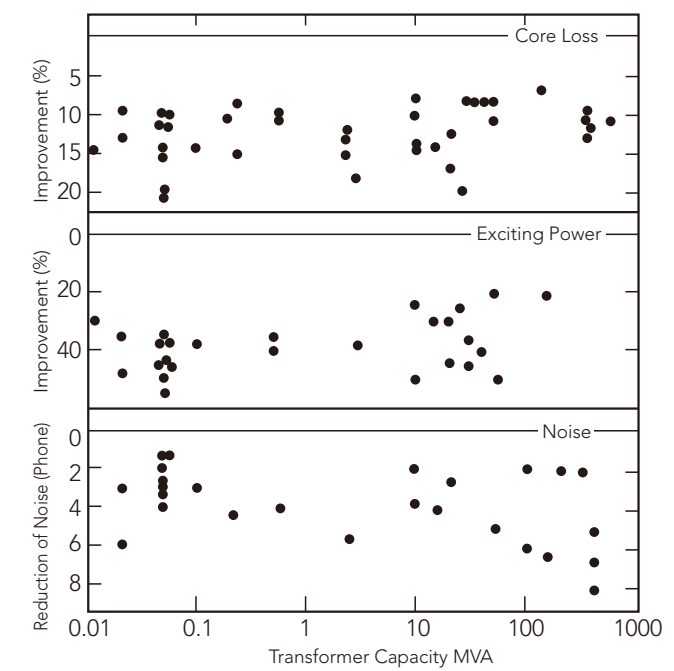


Fig. 2-1 Improvements in transformer characteristics.

3. Building Factor of Commercial Transformers

Building factors of single-phase and 3-phase 3-leg transformers classified by core structure are given in Figs. 3-1 and 3-2. There is no specific difference in the building factor of transformers with a 45°-joint regardless of whether they are made of ORIENTCORE·HI-B or C.G.O.. However in sheets with 90°-joints in the iron core, the building factor of ORIENTCORE·HI-B transformers is higher than that of C.G.O. transformers.

Fig. 3-3 shows building factors of 3-phase transformers with a special core structure (e.g., 3-phase 5-leg, shell type and other structures). A larger distortion of magnetic flux wave form is observed in the yoke zone of 3-phase 5-leg and shell type transformers, making the building factor higher. The above is the average value of the building factor. However, as shown in Figs. 3-1~3-3, individual building factors in fact vary considerably depending upon core structure, stack conditions, etc.

Note: Building Factor = $\frac{\text{Transformer Core Loss (W/kg)}}{\text{Material Core Loss (W/kg)}}$

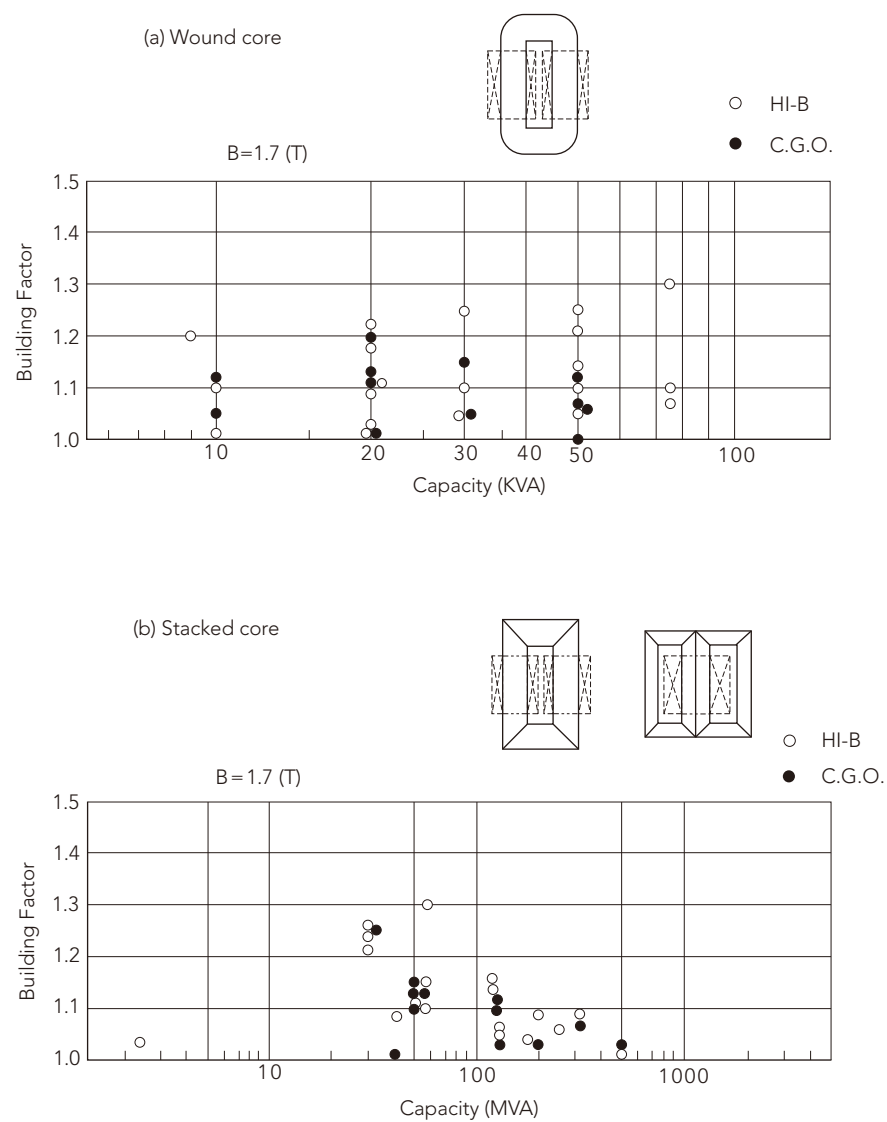


Fig. 3-1 Building factor of commercial single phase power transformers.

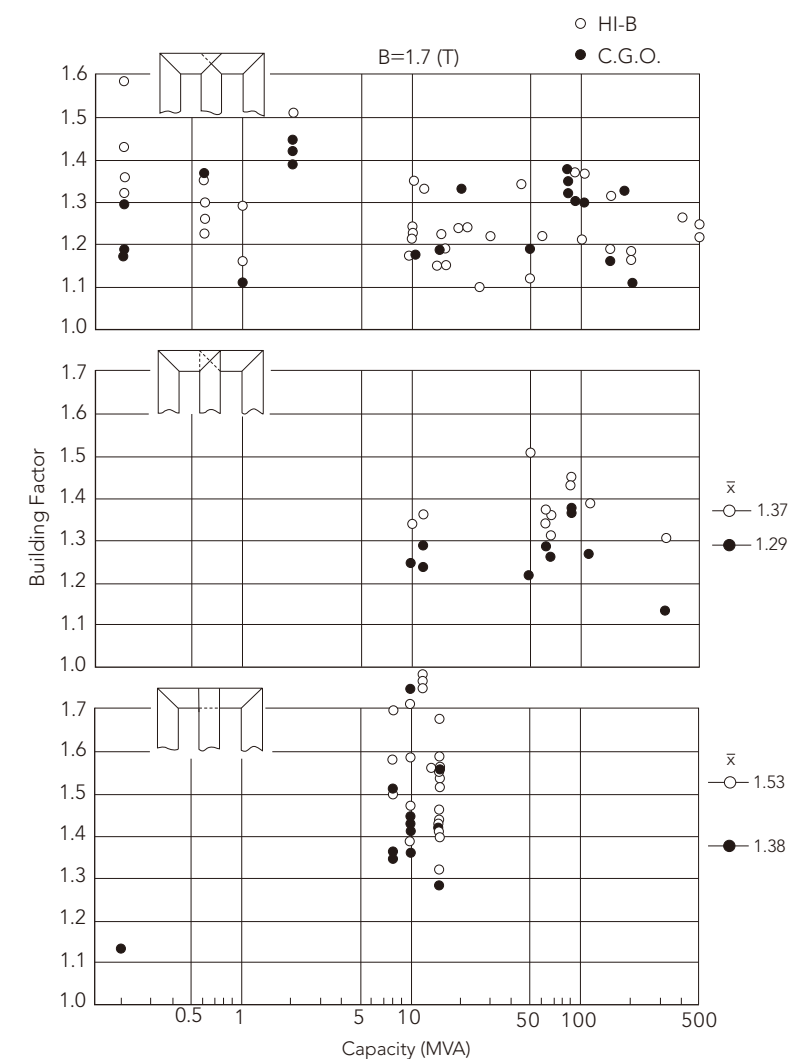


Fig. 3-2 Building factor of commercial power transformers (3φ-3 leg of core type)

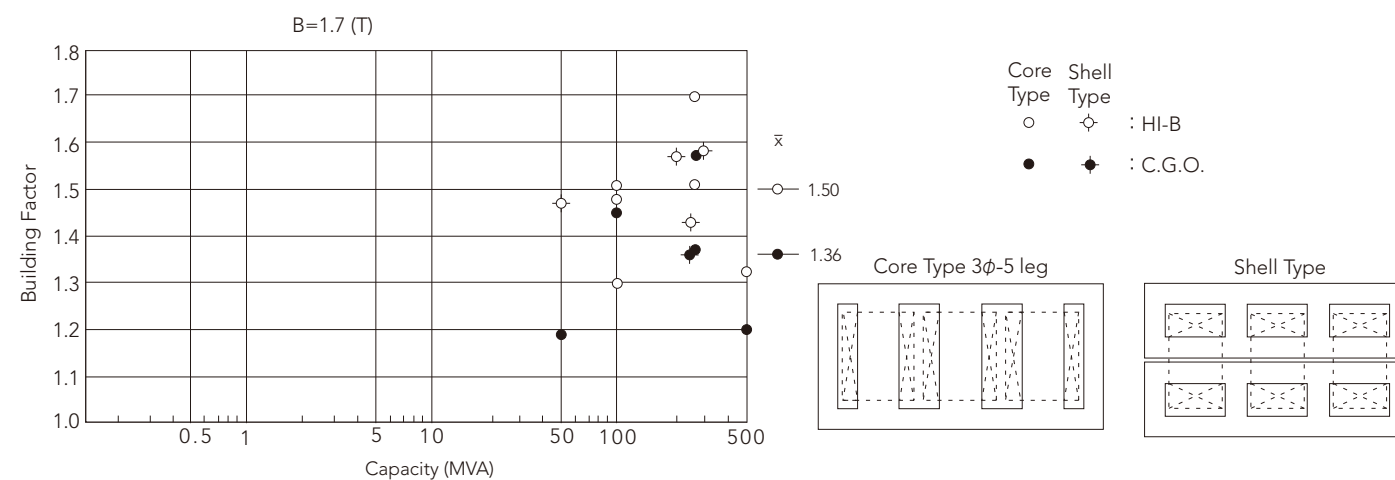


Fig. 3-3 Building factor of commercial power transformers (3φ-5 leg of core type and shell type)

4. Core Loss Characteristics of Model Transformer

4-1 Single-Phase Model Transformer

Fig. 4-1-1 shows the measured core loss of iron cores assembled with 45-joints. It has been proved that since most magnetic flux flows in the rolling direction, core loss is proportionate to the iron loss measured by the single sheet tester.

Fig. 4-1-2 shows the core loss measured with iron cores stacked with two different lap widths. It has been proved that in iron cores with 45-N joints, core loss and exciting volt-ampere increase with increasing lap width because of the effect of opening with a triangle shape in the corners, while in the case of 45-B-joints core loss and exciting volt-ampere remain almost constant.

4-2 3-Phase Model Transformer

A comparison of core loss between the 3-phase model and the single-phase model transformer is shown in Fig. 4-2-1.

Fig. 4-2-2 gives an example of local core loss measured by the Thermistor Bridge Method.

Values of core loss measured in T-joints and yoke zones are higher than that measured in the leg zone. This can be explained by the following three factors.

As generally known, core loss per unit weight in a 3-phase transformer is larger than that in a single-phase transformer. Presumable factors for the larger core loss are:

- 1) Core loss due to rotating magnetic flux in the region around T-joint Fig. 4-2-1, Fig. 4-2-3
- 2) Core loss due to magnetic flux in directions other than the rolling direction and magnetic flux concentration around lap joints Fig. 4-2-4
- 3) Core loss due to the lack of uniformity of magnetic flux caused by different magnetic path lengths and distortion of the magnetic flux wave form owing to the lack of uniformity Fig. 4-2-5 (a), (b)

As shown in Fig. 4-2-1~Fig. 4-2-5, an increase in magnetic flow in directions other than the rolling direction, polarization of magnetic flux, and partial distortion of magnetic flux wave form all make core loss higher.

Fig. 4-2-6 shows the relationship between the size ratio of the window and the building factor (transformer core loss/material core loss). The building factor decreases as the size ratio of the window increases. The rate of decrease is almost the same in both HI-B and C.G.O.

Due to transportation restrictions, the 3-phase, 5-leg type of iron core is often used in large-size transformer. This type of iron core is apt to cause a larger distortion of magnetic flux wave form in the yoke zone with a resulting higher core loss than with the 3-phase, 3-leg type of iron core.

Taking all factors mentioned above into consideration, the use of ORIENTCORE·HI-B in transformers can reduce both core loss and exciting current. In other words, the use of ORIENTCORE·HI-B in transformers assures better performance than does C.G.O.

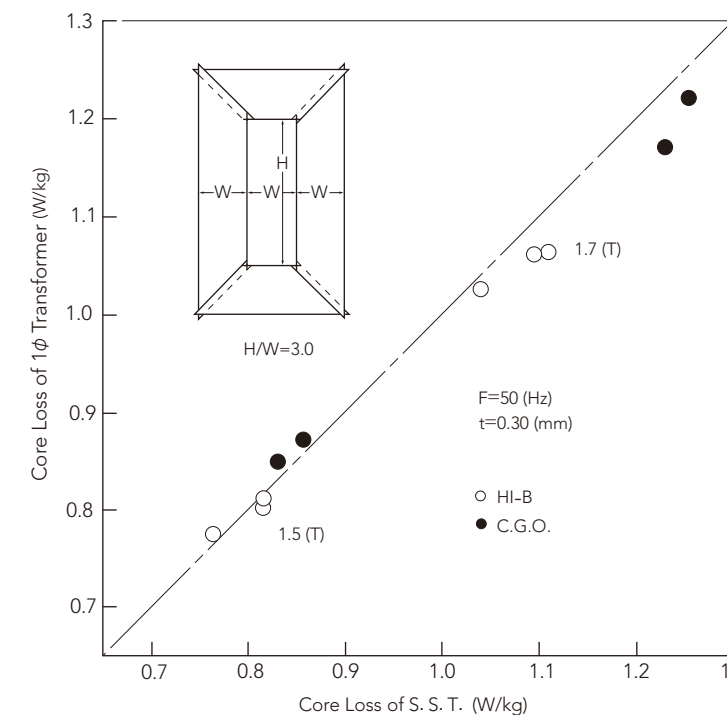


Fig. 4-1-1 Core loss characteristics of 45°-joint 1φ model transformer.

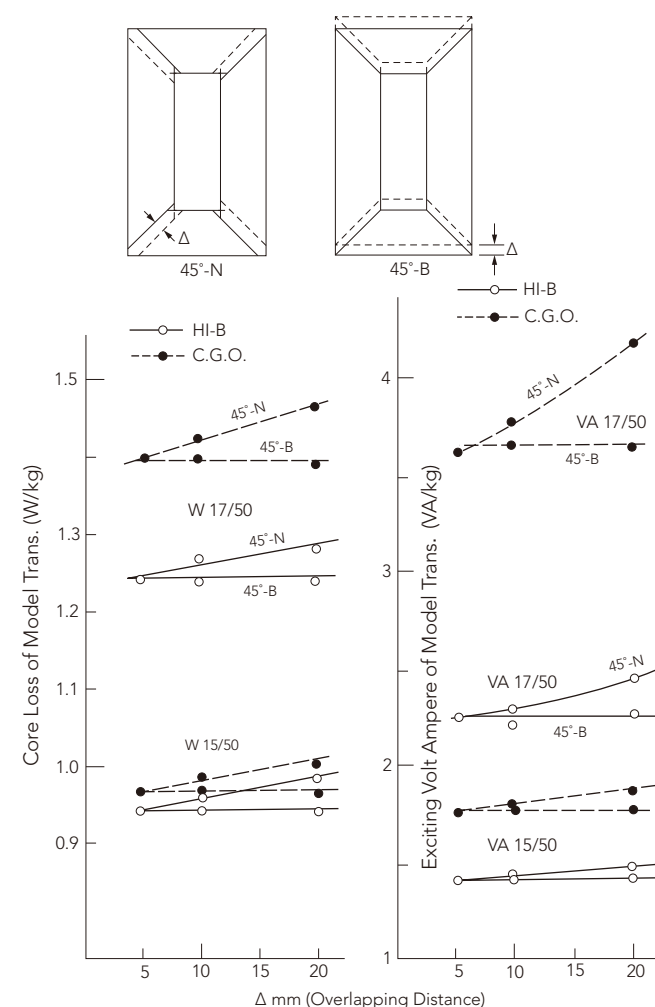


Fig. 4-1-2 Relationship between model transformer characteristics and the overlapping distance of lamination core.

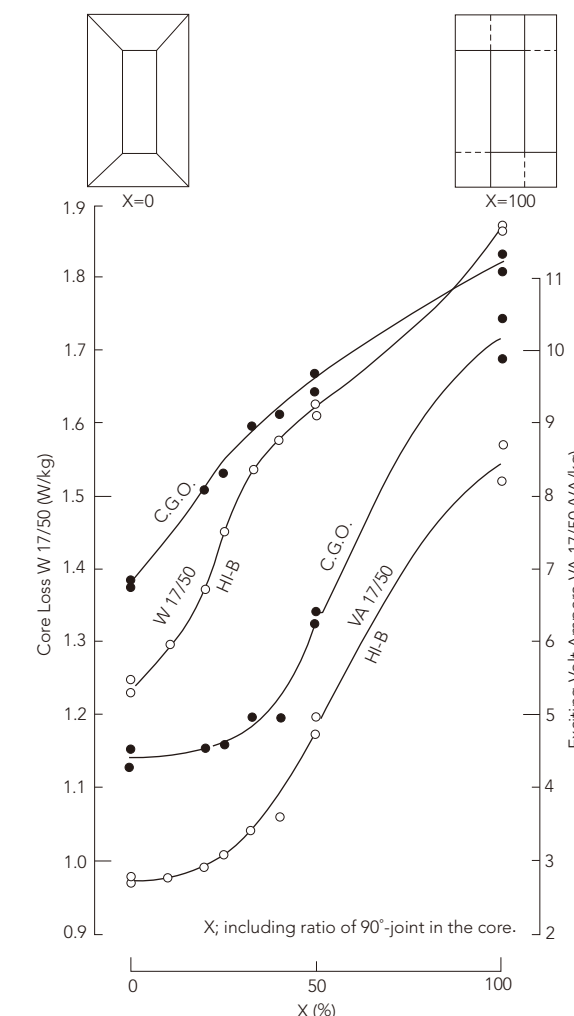


Fig. 4-1-3 Relationship between Model transformer characteristics and including ratio of 90°-joint in the core.

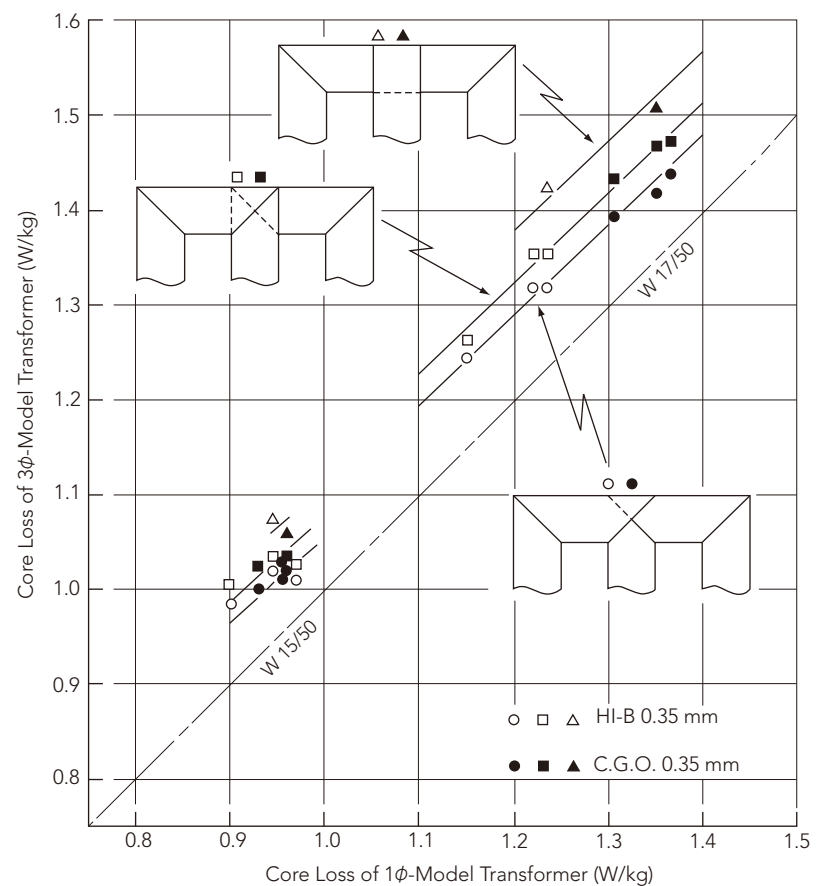


Fig. 4-2-1 Relations between core losses of 1φ and 3φ model transformers by different lamination methods.

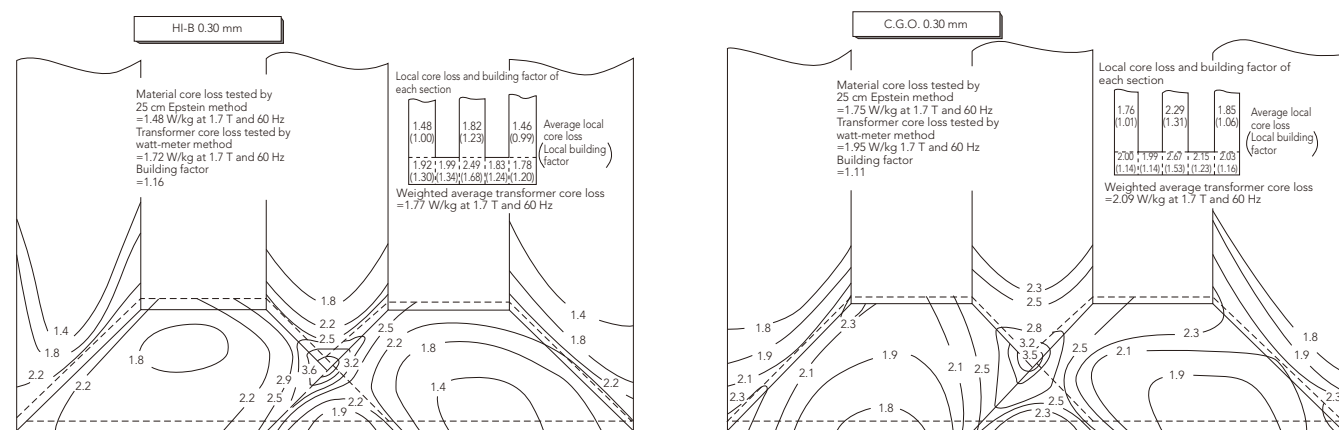


Fig. 4-2-2 Distribution of core losses in model transformer (local core losses were measured by means of thermistor bridge).

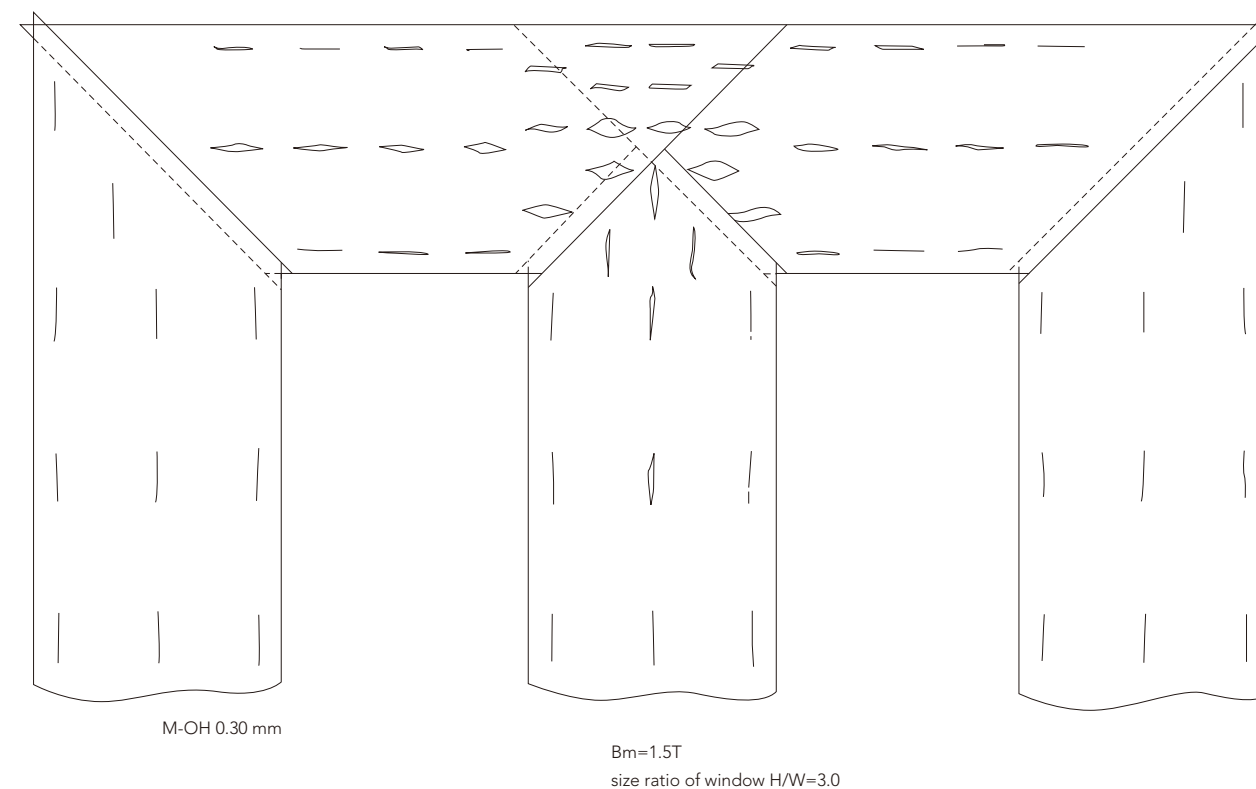


Fig. 4-2-3 Lissajous's figures of magnetic flux density in HI-B transformer.

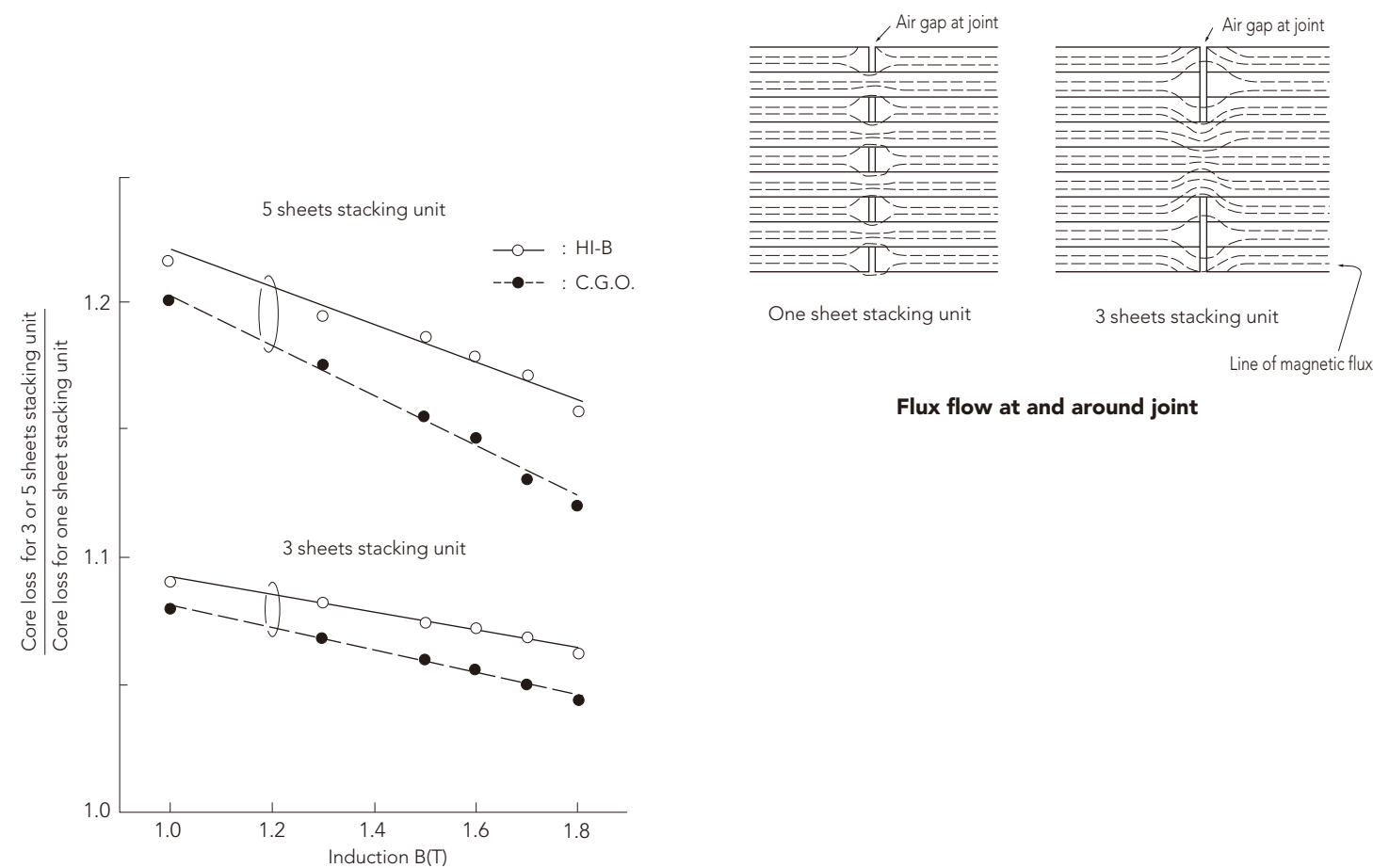


Fig. 4-2-4 The effect of lamination stacking unit on 3-phase transformer losses.

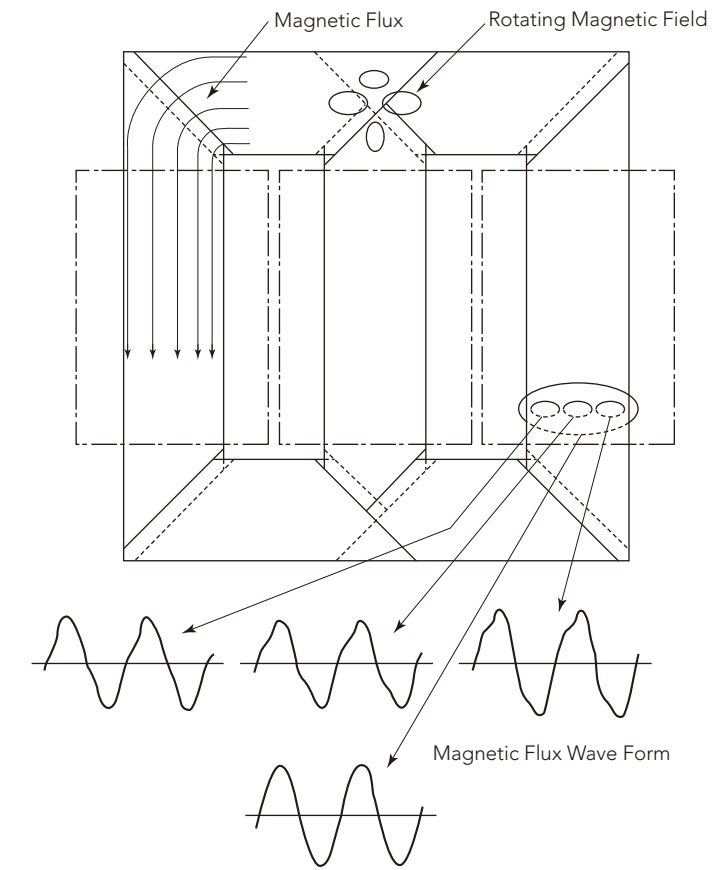
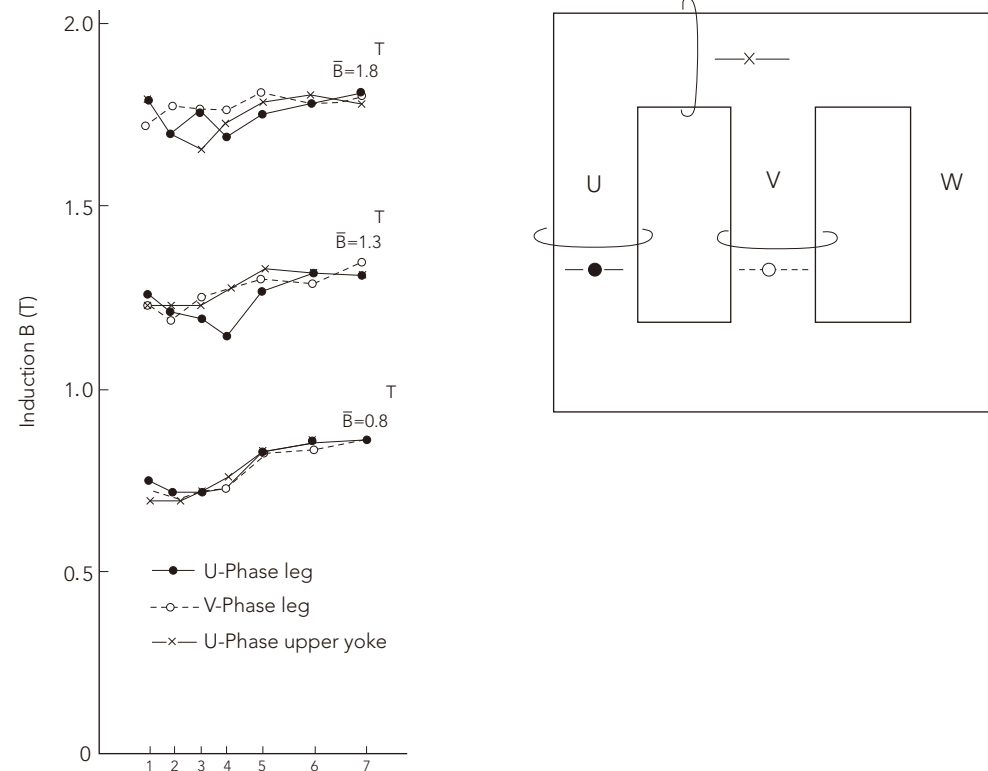


Fig. 4-2-5(b) Partial distortion of magnetic flux in model transformer.

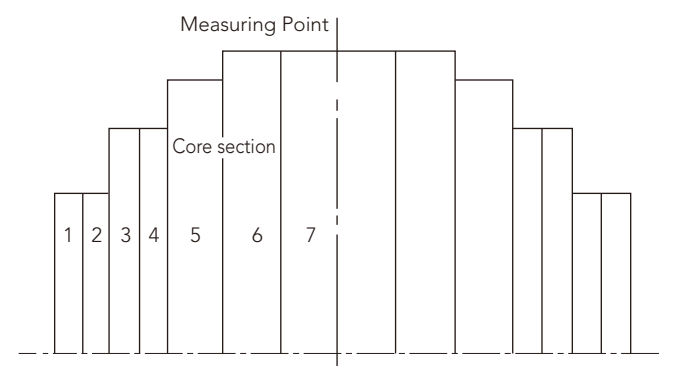


Fig. 4-2-5(a) Flux distribution in model core (Section: circle). Refer to TAKAOKA Review

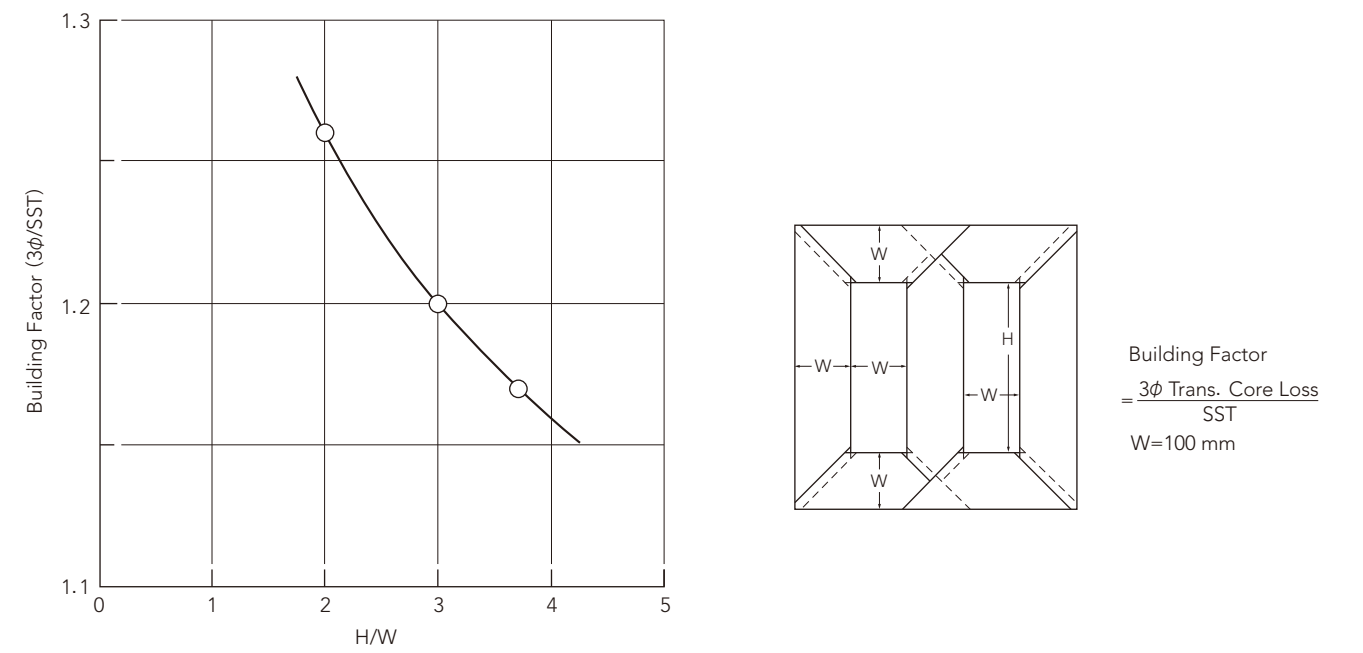


Fig. 4-2-6 The effect of H/W on building factor. H/W: size ratio of window.

APPENDIX [I]

A New Instrument for Measuring Local Core Losses Using Thermistor Bridge

1. Introduction

Electrical sheets do not necessarily become magnetized uniformly. Normally their magnetic properties such as intensity, orientation and magnetic flux wave form differ locally.

Although the mean iron loss of electrical equipment or electrical sheet is measured by use of a wattmeter, etc., some other method has to be employed for measuring local iron loss. For this purpose, we adopted a method which utilizes a thermistor and developed a local iron-loss measuring apparatus which incorporates a combination of AC thermistor bridges and a lock-in-amplifier.

This report describes our study of problems and the accuracy of measurement by this local iron-loss measuring apparatus, and finally, examples of applications are presented.

2. Measuring Apparatus

2.1 Principle of the Measuring Method

When a constant energy is applied to a substance under adiabatic conditions, its temperature rises linearly with the elapse of time at a rate determined by its heat capacity. If an electrical sheet is magnetized by AC, its temperature rises due to iron loss, and if the rate of its temperature rise is measured, its iron loss can be obtained.

The procedure for obtaining the absolute value of iron loss from the rate of temperature rise is as follows.

First, apply a DC to material identical to the specimen of iron loss measurement, and obtain the rate of temperature rise by the Joule heating.

Second, obtain the Joule loss per kilogram of the material from the value of the current and that of the resistance. Thus, by obtaining the relation between the Joule loss per kilogram of material and the rate of temperature rise, the iron loss per kilogram of material corresponding to the rate of temperature rise at the time of iron loss measurement can be calculated.

2.2 Configuration and Function of Measuring Apparatus

This apparatus consists mainly of a sensing unit, lock-in-amplifier, differentiator, Y-t recorder and measuring frame. Fig. 1 shows the configuration of the apparatus and Fig. 2 the typical arrangement of the thermistor of the sensing unit and measuring frame. The function of the apparatus is generally as follows. The thermistor is installed on the surface of the steel sheet and the bridge is adjusted to balance. When the thermistor senses any temperature change, the bridge balance is disturbed by the change in resistance, producing an unbalanced voltage. This unbalanced voltage is amplified by the lock-in-amplifier and synchronously rectified to obtain a DC output. This output is then differentiated by the differentiator, and recorded on the Y-t recorder whose X axis denotes time. As the rate of temperature rise becomes constant, the output voltage on the Y axis also becomes constant, and by reading this voltage, the rate of temperature rise is obtained.

As is shown in Fig. 1, two bridges, A and B, each having a thermistor and three resistors form the sensing unit, and are connected by wire so that bridges A and B function differentially. Hence, in order to prevent drift due to a change in ambient temperature, bridge B is used for compensation (as in the case of Fig. 2) and the temperature rise is measured employing bridge A. However, by the method of measuring the time differential of temperature change by the differentiator as done by this apparatus, even if a single bridge is employed, the effect of change in ambient temperature only produces an offset voltage working on the recorder if measuring is started when the change in ambient temperature becomes linear with time, and thus does not impede the proper function of the apparatus. An applied voltage adjusting resistor is installed in the bridge B circuit and adjusted to make the sensitivity of both bridges equal because it is difficult to obtain the same bridge characteristics for bridges A and B. The output and the differential output of each bridge are selected by switches.

3. Examples of Application of the Apparatus

3.1 Comparisons between This Measuring Method and the Wattmeter Method

A comparison was made using the same measuring frame for both this method and the wattmeter method in measuring the iron loss of a single electrical sheet specimen. The construction of the measuring frame is shown in Fig. 3, and the frame is sealed in a bakelite box to eliminate the direct effect of atmospheric air. Also, to prevent the specimen from coming into contact with the bakelite of the coil frame, it is held up by the insertion of a styrofoam board. The thermistor sensor is embedded in the styrofoam except for the portion in contact with the steel sheet to shield it against heat radiation from the coil. A dummy specimen was placed in the same heat-shielded box, and the double bridge method was used. The specimen for measuring was 6 cm wide, 30 cm long and 0.028 cm thick. The wattmeter method is capable of measuring iron loss over a broad area. In this measuring method, an average of 15 point measurements are taken, at 3 locations separated 6 cm from each other in the middle in the longitudinal direction and at 5 locations at 1 cm intervals in the transverse direction. The result of the measurement is shown in Fig. 4. From this graph it is clear that the measurements of both methods are in good agreement. The same magnetic flux density of 0.5~1.5 T was adopted in measuring iron loss.

3.2 Measurement of 3-Phase Model Transformer Iron-Loss Distribution

Iron loss was measured by this apparatus at locations on a small model of core-type 3-phase transformer. The measuring frame used had the construction shown in Fig. 5, and considerations were given to eliminate the effect of atmospheric air and assure heat insulation, just as in the foregoing case.

Shown in Fig. 6 is a distribution of iron loss measured by the use of this apparatus, and the distribution is indicated by equal iron-loss lines. The measurement was conducted at 10 mm intervals on the top of a 12-layer specimen block of oriented electrical sheets. The iron loss of the entire transformer calculated using this result was $W_{17/60} = 1.77$ W/kg, and that obtained by the wattmeter method was $W_{17/60} = 1.72$ W/kg, showing a comparatively good agreement between them.

4. Conclusion

The local iron-loss measurement is a very useful means of studying the magnetic properties of electrical sheets. In this respect, it is necessary to carry out measurements accurately with high stability. We have made it possible to obtain high stability by a combination of AC thermistor bridges and a lock-in-amplifier, and to achieve the shortening of test time as well as the improvement of accuracy by directly measuring the rate of temperature rise by the use of a differentiator.

APPENDIX [II]

Various Core Stacking Types (3φ)

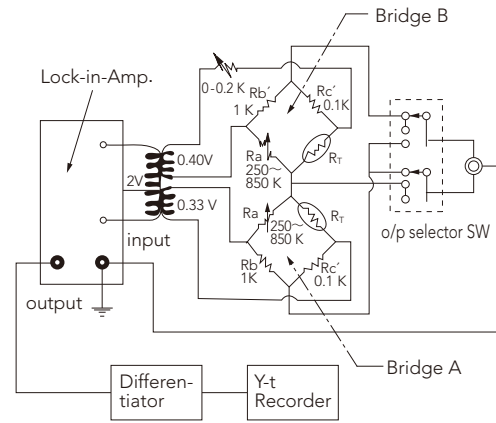


Fig. 1 Block-diagram of apparatus.

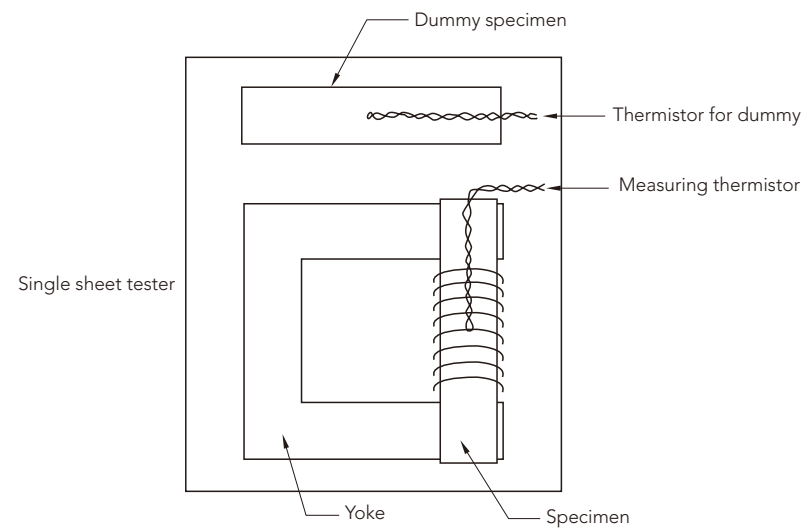


Fig. 2 Example of measuring frame and thermistor arrangement.

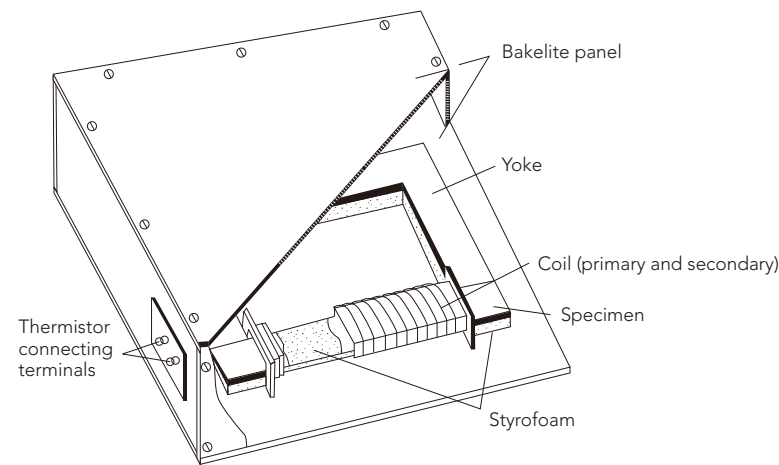


Fig. 3 Measuring frame for single steel sheet.

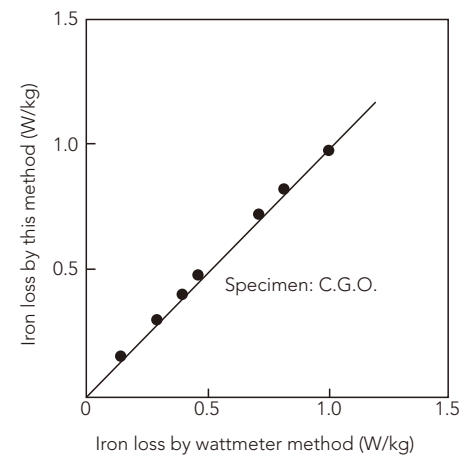


Fig. 4 Comparison of core losses measured by this method and wattmeter method.

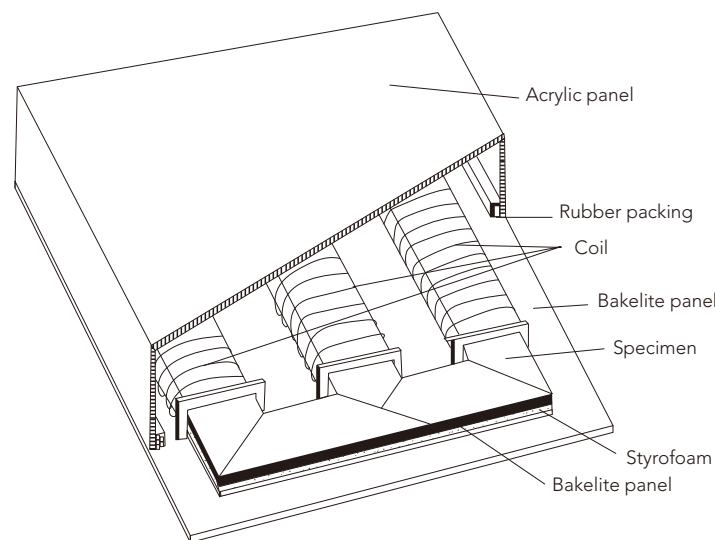


Fig. 5 Measuring frame for small three phase model transformer

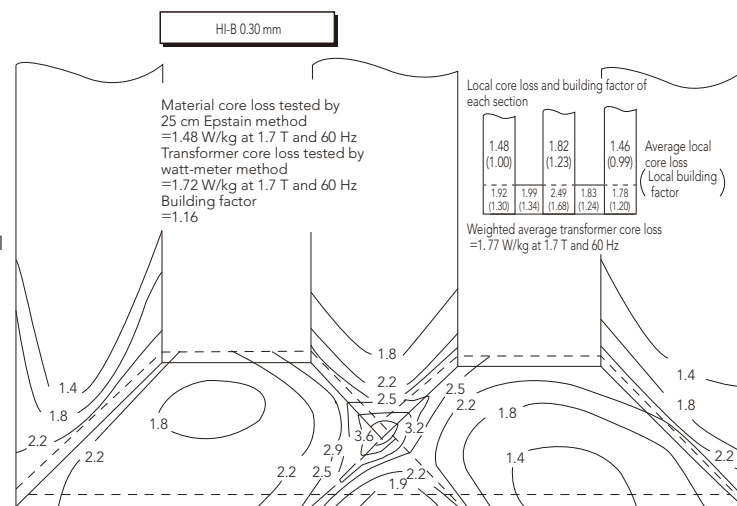
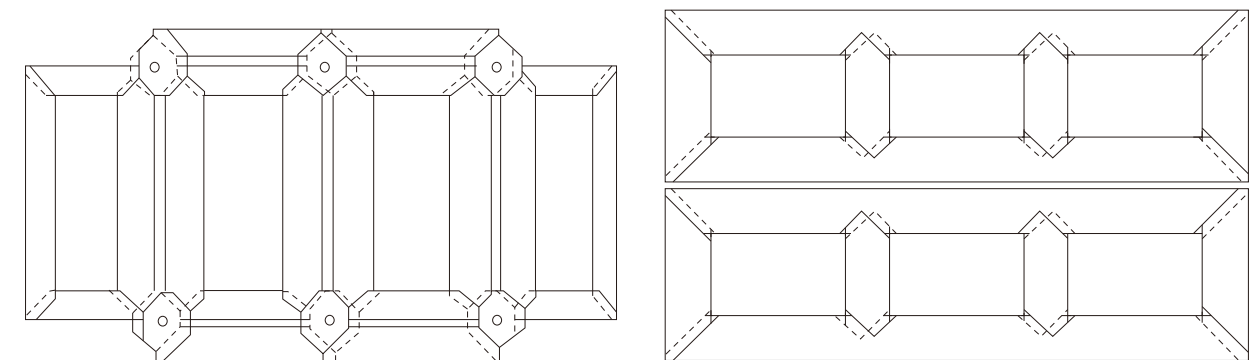
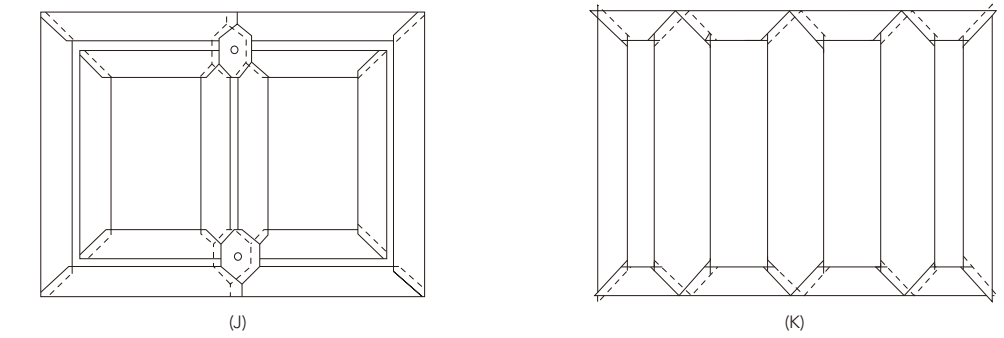
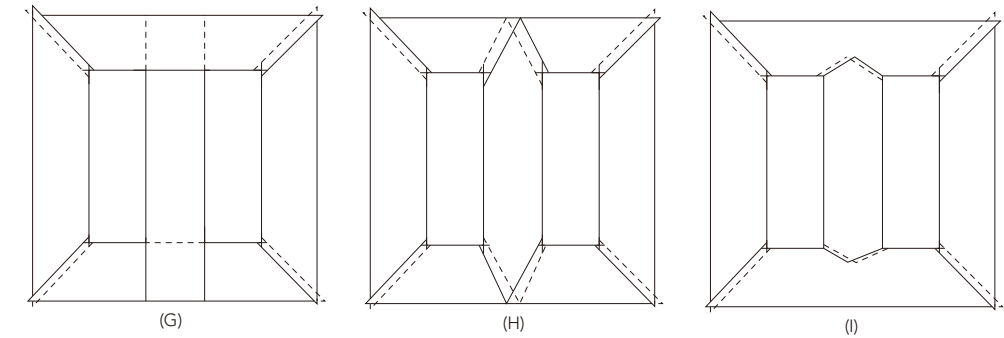
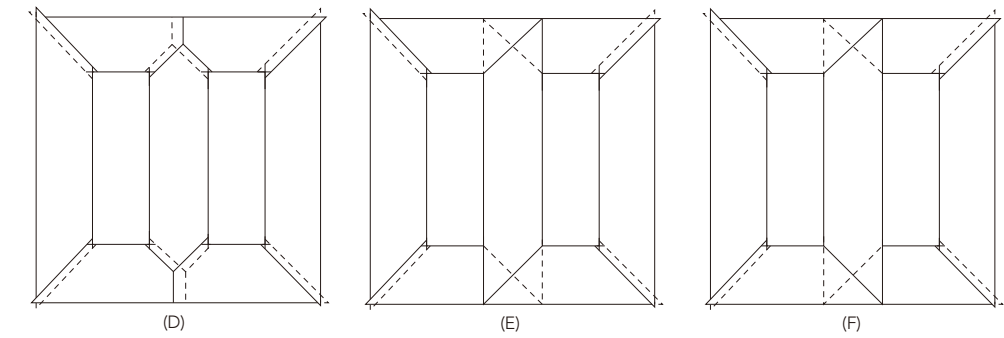
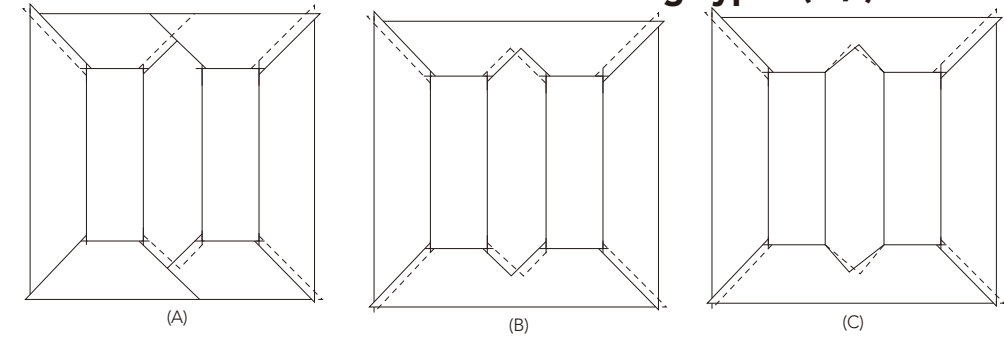


Fig. 6 Distribution of core losses in model transformer.



APPENDIX [Ⅲ]

Mechanical and Physical Properties of HI-B And C.G.O.

		HI-B	C.G.O.
Tensile Strength, kg/mm ² (lb/m ²)	L	32 (46,000)	36 (51,000)
	C	38 (54,000)	40 (57,000)
Yield Point, kg/mm ² (lb/m ²)	L	30 (43,000)	32 (46,000)
	C	33 (47,000)	40 (55,000)
Elongation, %	L	13	17
	C	64	65
Bending, Test Values	L	28	18
	C	18	14
Modulus of Elasticity, ×10 ⁴ kg/mm ²	L	1.189	1.114
	C	2.038	1.931
Hardness, Hv (1)		170	175
Density, g/cm ³		7.65	7.65
Resistivity, micro-ohm-cm		45	48
Saturation Induction, Tesla		2.03	2.03
Curie Temperature, °C		745	745
Thermal Conductivity at 25°C, cal/sec. cm. deg.°C		0.067	0.061

L=Test specimens taken longitudinal to the rolling direction

C=Test specimens taken transverse to the rolling direction

Note: Tensile and bend tests were conducted in accordance with JIS C 2550 1975.